RADIO FREQUENCY TRANSMISSION SYSTEM A 30 MEV ELECTRON CYCLOTRON

M. Innas Ali

Physics Department, Dacca University, Dacca, East Pakistan

THE principle of magnetic resonance in which the operation of an electron cyclotron rests has been discussed in great detail by various authors since its introduction by Veksler (Veksler,[1] Readhead et al.,[2] Henderson et el.,[3] Itoh and Kobayshi[4]). It consists essentially of a resonant cavity situated in a uniform magnetic field. The cavity is energized by a pulsed magnetron.

A very high electric field is obtained across the lips of the cavity. The electrons obtained by field emission from the lips of the cavity and accelerated each time they pass through the cavity describe orbits of increasing radius which all have a common tangent through the resonator.

The radio frequency system of the electron cyclotron consists mainly of three parts : (a) the R.F. source ; (b) the R.F. transmission system ; and (c) the cavity resonator.

The R.F. source is a high power pulsed magnetron with a conventional modulator unit. This paper describes the development and design of an efficient R.F. transmission system for feeding power stably from the magnetron to the cavity resonator.

Magnetron Stabilization

If the magnetron is coupled to a waveguide terminated in a resonant load the input impedance under cold condition may be represented by

$$Y_L(w) = G(w) + jB(w) \quad - - - (1)$$

where (w) is the angular frequency, G(w) represents the conductance and B(w) the susceptance. G(w) and B(w) can be determined in terms of the admittances of the magnetron cavity and load and the waveguide constants.

Fig. (1) shows B(w) as a function of G(w) at different frequencies in the complex plane. $Y_L(w)$ at any frequency can be found from this curve.

When the magnetron is under operating conditions, new admittances are introduced

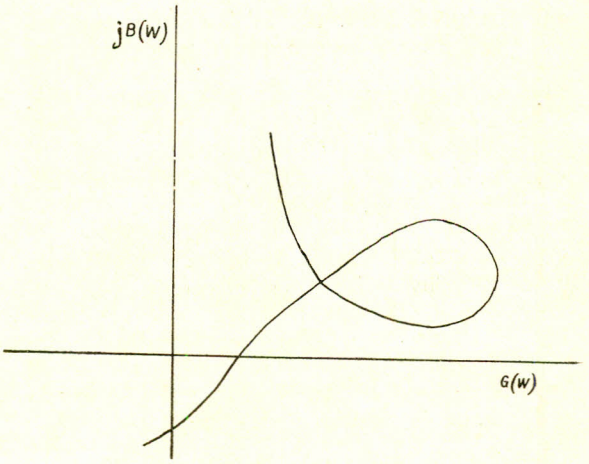

Fig. 1

due to electron loading in the magnetron. We represent this admittance as Y_e. When $Y_e = -Y_L$ the total input admittance of the magnetron is zero and this is the condition for maintaining oscillations. The admittance Y_e depends on the voltage and current applied to the electron stream and other input states such as temperature, etc. We shall assume that the Y_e curves are straight horizontal lines parallel to the real axis, when represented in the G-B plane. In general, Y_e curves may intersect the Y_L curves at more than one point, indicating that $Y_L = -Y_e$ at more than one frequency, and the magnetron is capable of oscillating at more than one frequency not all of them, however, are stable. In practice, the magnetron does not oscillate at two frequencies simultaneously. This must mean either that there is involved some sort of selection process which operates in favour of one or the other of the intersections or that simultaneous oscillation at two frequencies is an inherently unstable state.

The most natural way to describe the operation of a magnetron is in terms of its Ricke diagram, which is a plot on a circle impedance diagram of its performance (output power and frequency) for loads of all possible impedances. If the load is critical to frequency, as in the case of a resonant cavity and if its impedance is plotted as the frequency is varied,

a curve will be obtained on the chart. Possible operating points, if any, will be at points where the magnetron frequency contours intersect the load curve at their own frequency.

When the magnetron is switched on, there is nothing to choose between the various possible modes, and they will all be present at very low amplitude. Due to the non-linear characteristics of the oscillator, the operating condition with the most rapid rate of build-up of oscillation will be the one in which the steady-state is reached, to the exclusion of all other modes. The mode of most rapid build-up is normally that of lowest equivalent Q-factor.

Unfortunately the build-up of oscillation at the resonant frequency of the cavity has the slowest rate.[5] If other modes are possible, oscillation will not take place at the resonant frequency, hence if operation is desired at the resonant frequency, it must be the only mode which fulfils the stability requirements. The method of suppressing the unwanted modes is to ensure that both the admittance and the impedance of the load remain less than certain critical values dependent on the characteristics of the oscillator at frequencies remote from the resonant frequency of the load. In other words, it is necessary to dissipate some of the power in a load so that the resonance curve is displaced towards the centre and made symmetrical with respect to the magnetron frequency contour equal to the resonant frequency of the cavity. There are several methods by which this can be done ; we shall discuss two of them which are most practical :

(1) A resistive load is inserted either in series with the transmission line at an integral number of half-wavelengths from the resonator input, or in parallel at an odd number of quarter-wavelengths from the resonator. The minimum value of this load depends largely on the character of the Ricke diagram of the oscillator. The arrangement is called 'point load stabilization'.

(2) An attenuator with some suitable transformer is inserted in the transmission system. The arrangement is called 'attenuator load stabilization'.

Point Load Stabilization

For mechanical reasons, the stabilizing load is placed in series with the transmission line at an integral number of half-wavelengths from the resonator input. This is done by coupling the stabilizing load to the main wave-guide through an E-plane series T-junction. In such a junction, the discontinuities in the guide give rise to storage fields, the effects of which may be represented by lumped susceptances. The numerical values can be determined from the wave-guide dimensions, using the empirical information collected by Huxley.[6] The stabilizer resistor is a matched water load. The inductive susceptances in the main arms of the T-junction are considered to be small enough not to require compensation. Two appropriately placed screws ahead of the water load can be used to adjust the load to its optimum value and to cancel the shunt susceptance at the side-arm introduced into the wave-guide by the T-junction. Figure 2 shows the layout of the stabilizer. The whole stabilizer system can be represented as a damping resistor in series with the cavity. The cavity plus this resistor now represents the load.

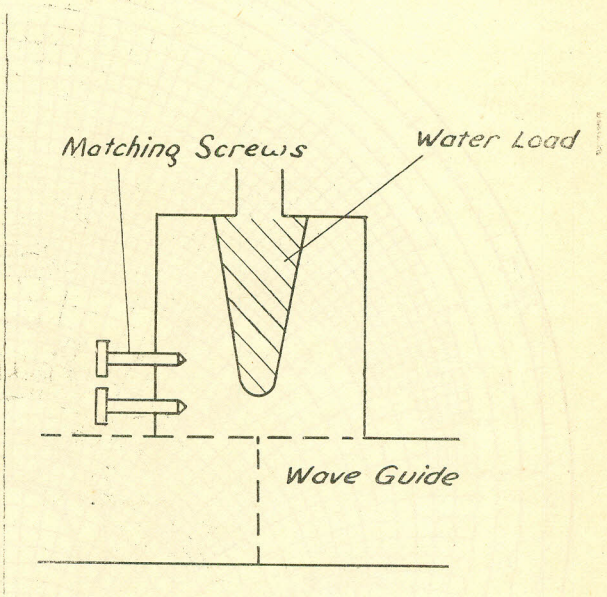

Fig. 2

The effect of the damping resistor in suppressing the extraneous modes can be analyzed by means of admittance curves in a reflection coefficient diagram (Smith chart) which are called circle diagrams. If the off resonance region of circle diagram of the cavity plus stabilizing resistor is sufficiently displaced towards the centre of the Smith chart there will be one and only one operating point which can be adjusted to be at the resonant frequency of the cavity. In addition it is advantageous to arrange for the circle diagram to be symmetrical with respect to the centre of the impedance diagram, since then the magnetron

would operate into a load of constant voltage standing wave ratio irrespective of mis-adjustment of the resonator frequency.

Circle diagram of point-load plus loaded cavity:

Let R_s = Series resistance introduced by point load.

R_c = Cavity shunt resistance.

Z_o = Characteristic impedance of wave-guide.

$$R_1 = \frac{R_s}{Z_o} \text{ and } R_2 = \frac{R_c}{Z_o}$$

on-tune V.S.W.R., $S_o = R_1 + R_2$.

on-tune reflection coefficient,

$$P_o = \frac{R_1 + R_2 - 1}{R_1 + R_2 + 1}$$

Off-tune reflection coefficient,

$$P_{off} = \frac{R_1 - 1}{R_1 + 1}$$

Circle diagram of point load plus unloaded cavity:

Let R_E = Shunt resistance introduced due to electron beam loading in the cavity

and $f = \frac{R_c}{R_E} = \frac{\text{Beam power}}{\text{Wall losses}}$

on-tune reflection coefficient,

$$P_{ol} = \frac{(R_1+R_2-1)+f(R_1-1)}{(R_1+R_2+1)+f(R_1-1)} \qquad (2)$$

off-tune reflection coefficient,

$$P_{ofl} = P_{off} = \frac{R_1-1}{R_1+1}$$

Circle diagrams of point load plus loaded and unloaded cavity are drawn in Fig. 3.

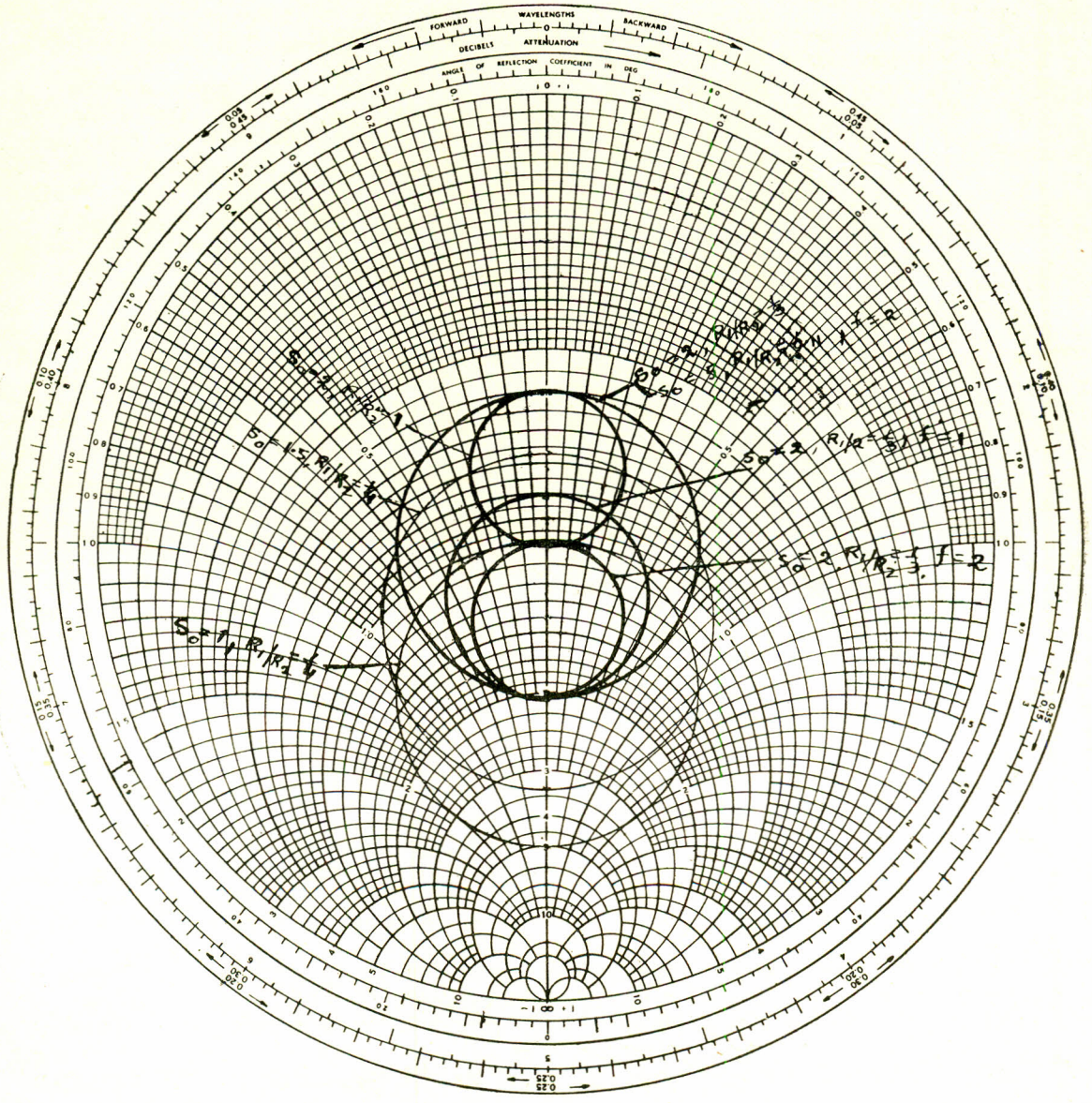

Fig. 3

Power relations in a point load stablizer system

Power dissipated in resonator and electron beam

$$= V_R^2 \frac{(R_E+R_C)}{R_E R_C}$$

Resultant input power

$$= V_R^2 \frac{(R_C+R_E)}{(R_C R_E)^2} \quad (R_C R_E + R_S R_C + R_E R_S)$$

put $$f = \frac{R_C}{R_E} = \frac{\text{Power in beam}}{\text{Power in resonator walls}}$$

and $$F = \frac{\text{Input power}}{V_R^2/R_C} = \frac{\text{Input power}}{\text{Power in resonator walls}}$$

Then $$F = \left[f+1\right]\left[1+\frac{R_S}{R_C}(1+f)\right] \quad .. \quad .. \quad (3)$$

Normalizing R_S, R_C and R_E we get

$$R_1 = \frac{R_S}{Z_0} \quad R_2 = \frac{R_C}{Z_0} \quad R = \frac{R_E}{Z_0}$$

and

$$F = (f+1)\left\{1+R_1/R_2\,(1+f)\right\} \quad .. \quad .. \quad (4)$$

Groups of F v s f for point load system are shown in Fig. 4.

Attenuator—load stabilizer

Theoretical analysis: The general arrangement of the R.F. transmission system with the attenuator load is shown in Fig. 5 and the equivalent circuit is shown in the inset to Fig. 5.

We shall consider the circle diagrams as measured at terminals C-C (Inset Figure 5). The quarter-wave transformer is of characteristic impedance r_0. The attenuator has the same characteristic impedance Z_0 as the

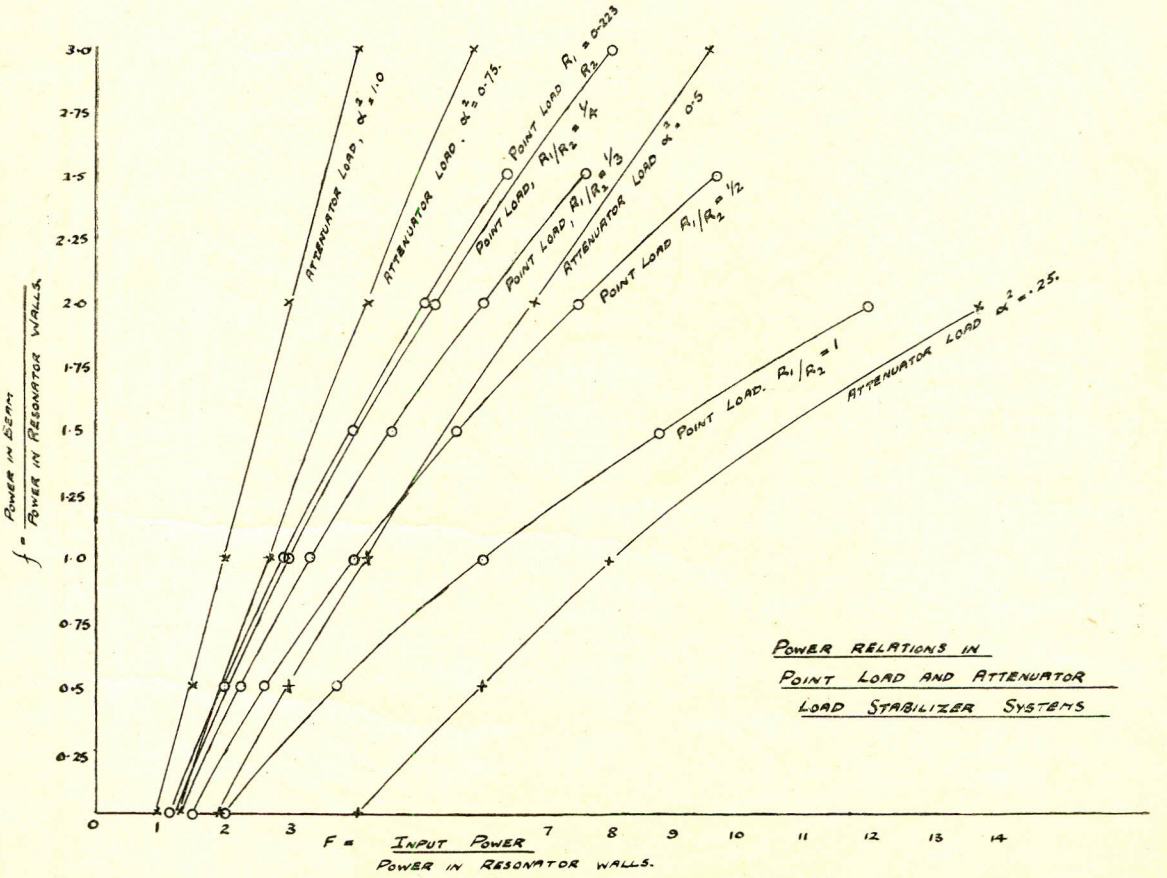

Fig. 4

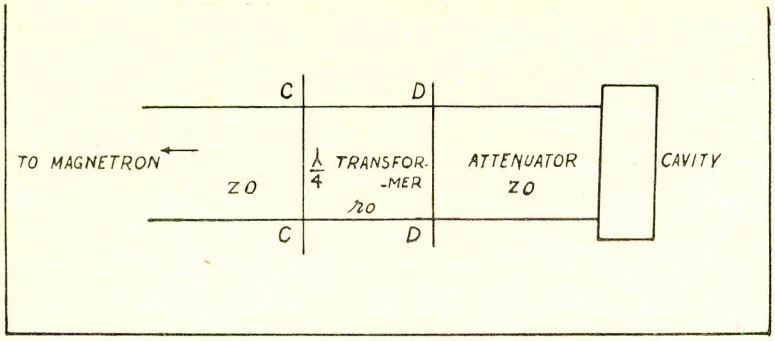

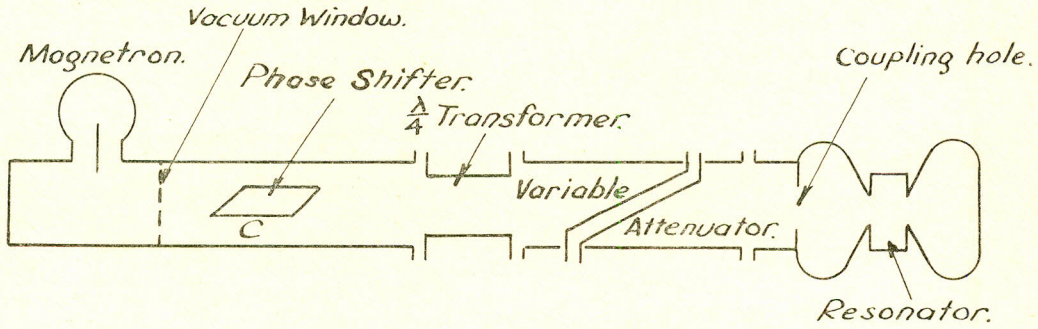

Fig. 5. R. F. Transmission system

waveguide and is an integral number of half-wavelengths. Let the attenuator reduce the field in passing through it by a fraction α.

Let the on-tune reflection coefficient for the unloaded cavity be P_0. Assuming no phase change by the attenuator, the on-tune reflection coefficient at the attenuator input= $\alpha^2 P_0$.

On-tune V.S.W.R. at attenuator input $= \dfrac{1-\alpha^2 P_0}{1-\alpha^2 P_0}$

Off-tune reflection coefficient at unloaded cavity $= -1$

Off-tune reflection coefficient at attenuator input $= -\alpha^2$

Off-tune V.S.W.R. with no load at attenuator input

$$= \frac{1-\alpha^2}{1+\alpha^0}$$

As the attenuator is an integral number of half-wavelengths, the on-tune input impedance at attenuator input (Terminals D-D) is R_C and the off-tune impedance is jx_C (neglecting change in electrical length due to change of frequency.

On-tune V.S.W.R. at attenuator input if there were no transformer

$$S_o = \frac{1+\alpha^2 P_0}{1-\alpha^2 P_2}$$

Off-tune V.S.W.R. at attenuator input without transformer

$$S = \frac{1-\alpha^2}{1+\alpha^2}$$

On tune V.S.W.R. at transformer input (Terminal C-C) is given by

$$S_{on} = \frac{r_o^2}{Z_o^2 S_o} = \frac{n^2}{S_o}$$

where $n = \dfrac{r_o}{Z_o}$

Off-tune V.S.W.R. at transformer input is given by

$$S_{of} = \frac{Z_o^2 S}{r_o^2} = \frac{n^2}{S}$$

On-tune reflection coefficient at transformer input

$$P_{on} = \frac{\frac{n^2}{S_o^2} - 1}{\frac{n^2}{S_o^2} + 1} = \frac{(n^2-1) - \alpha^2 P_o (n^2+1)}{(n^2+1) - \alpha^2 P_o (n^2-1)} \quad \ldots (5)$$

Off-tune reflection coefficient at transformer input

$$P_{off} = \frac{\frac{n^2}{S} - 1}{\frac{n^2}{S} + 1} = \frac{(n^2-1) + \alpha^2 (n^2+1)}{(n^2+1) + \alpha^2 (n^2-1)} \quad \ldots (6)$$

we have $P_o = \frac{R^2 - 1}{R^2 + 1}$ for unloaded cavity

$$P_{lo} = \frac{2P_o - f(1 - P_o)}{2 + f(1 - P_o)} \text{ for loaded cavity}$$

In this analysis we are assuming that the electrical length of the attenuator remains constant at an integral number of half-wavelengths, while the transformer remains quarter-wavelengths over the whole frequency range. This is nearly true since we are dealing with a small frequency range. If the length of the attenuator is not an integral number of half-wavelengths the circle diagram will be rotated bodily and some deformation of the curve from its circular form, which is not at all serious for practical purposes, will result. The circle diagram can, however, be brought back to its original position by means of some suitable phase shifter introduced into the transmission system.

Circle diagrams for attenuator load system plus cavity are shown in Fig. 6.

Power relation in an attenuator load stabilizer system.

Power input varies as $(1 - P^2 \alpha^4)$

where P is the reflection coefficient at cavity input.

At resonant frequency total power absorbed by resonator varies as

$\alpha^2 (1 - P^2_{LO})$

Resonator power division

$$\frac{P_{beam}}{P_{wall}} = \frac{\text{Power in Beam}}{\text{Power in Wall}} = f$$

$P_{wall} + P_{beam}$ varies as $\alpha^2 (1 - P^2_{LO})$

or, $$1 + f = \frac{\alpha^2 (1 - P^2_{LO})}{P_{wall}}$$

or, $$P_{wall} = \frac{\alpha^2 (1 - P^2_{LO})}{1 + f}$$

$$\frac{\text{Power input}}{\text{Power in Wall}} = F = \frac{(1 - P^2_{LO} \alpha^4)\ (1 + f)}{\alpha^2 (1 - P_{LO}^2)} \quad (7)$$

Graphs of F V S f are also shown in Fig. 4.

Discussion of results and comparison of the performance of the two systems : The study of the circle diagrams in Figure 3 reveals that the point load stabilizer system with an unloaded cavity has a symmetrical circle diagram for $R_1/R_2 = 1/3$ with $R_2 = 1.5$ and the V.S.W.R. as seen by the magnetron is 2 at all frequencies. When the cavity is loaded with f = 2 off-tune standing wave ratio remains the same ; but the on-tune standing wave ratio is considerably reduced.

A slightly better circle diagram (Figure 6) is given by the attenuator system with unloaded cavity for $\alpha^2 = 0.5$, with $R_2 = 1.5$ and $n^2 = 0.64$ and the V.S.W.R. is nearly 1.9 at all frequencies. Keeping the off-tune V.S.W.R. the same, the cavity loading again reduces the on-tune V.S.W.R. The circle diagrams illustrate the point that any circle diagram which can be produced by a point load system can also be produced by an attenuator system by a proper choice of the attenuation and the quarter-wave transformer.

The study of Figure 4 shows that for values of beam loading in accelerator cavity upto about three times the wall losses the circuit efficiency is slightly better in the point load system than in the attenuator system. Normally, the beam loading is twice the resonator wall losses and hence the point load system compares favourably with the attenuator system so far as power relations are concerned. This slight advantage in power relations in the point load system, is however more than offset by difficulties in its design and operation. It is not possible to compensate all the reactances and susceptances associated

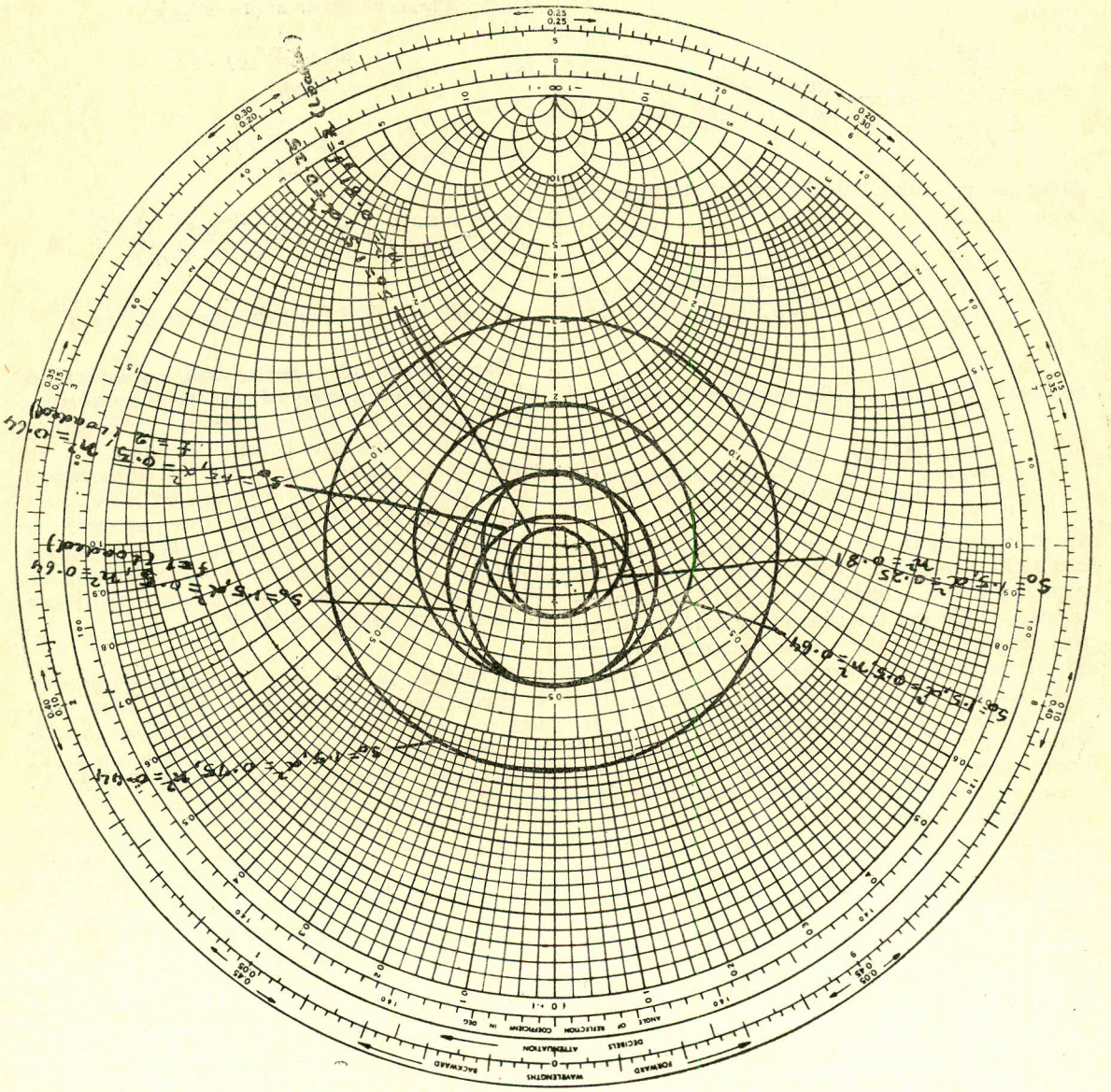

Fig. 6

with the point load, nor is it possible to *continuously* vary this load for operational adjustments. Moreover, we do not know the Ricke diagram of the magnetron. If we use a point load, we have to guess the minimum value of the stabilizing resistor, and we will almost certainly make it too large in order to be on the safe side.

An attenuator can, however, be easily designed and constructed with means of adjustments during operation.

Attenuator Load

A variable evacuated attenuator load was designed and constructed in the laboratory and its performance was studied experimentally with a view to using it in an attenuator transmission system in the electron cyclotron. The general arrangement of the attenuator load is shown in Figure 7 and Plate I. It is a variable

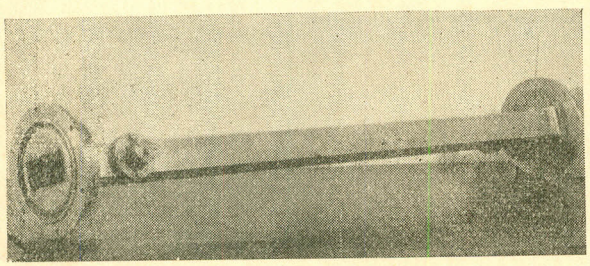

Plate 1

water load attenuator with a glass tube passing through a wave-guide at a slanting angle. The attenuation is varied by varying the level of water inside the tube as shown diagrammatically in Figure 8.

The glass tube is bent at right angles at both ends, which come out of the waveguide through two vacuum-sealed assemblies on top and bottom faces of the waveguide. Water is slowly dripped in from water mains to the top end of the glass tube and comes out through the bottom end, which is connected to one end of a rubber tube, the other end of which carries a glass tube placed vertically along a millimetre scale to read its top head. By sliding the glass tube up and down the water level inside the waveguide can be adjusted.

Attenuation was measured for different water levels inside the attenuator by the standing wave ratio method. The circle diagrams of the attenuator terminated by the cavity for different attenuation constants were also determined from the standing wave

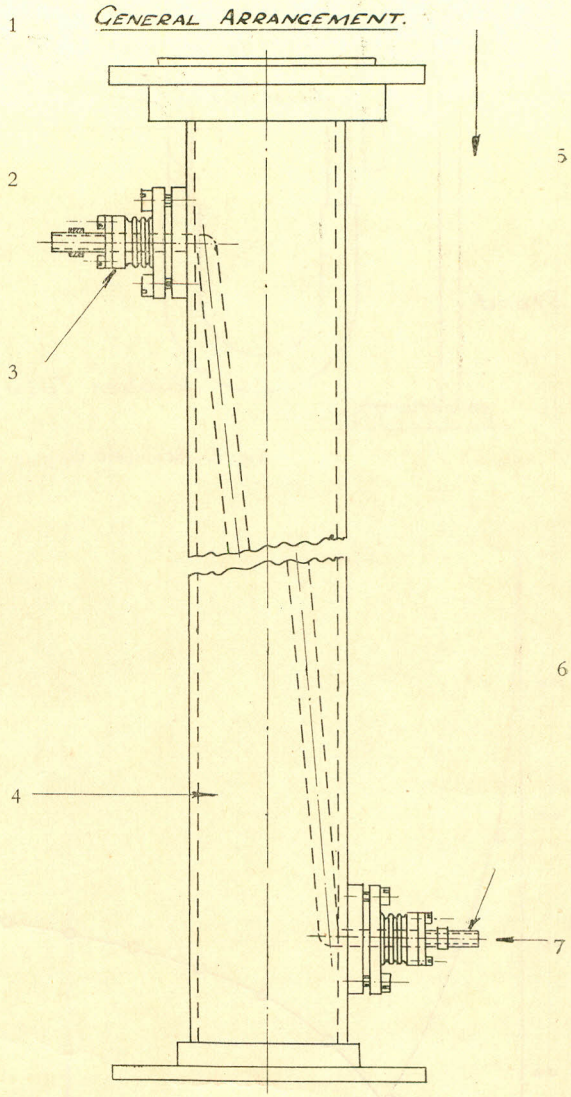

1 Water Load
2 Variable Attenuator
3 Outlet Assembly
4 Wave-guide
5 Power In
6 Glass Tube
7 Water In

Fig. 7

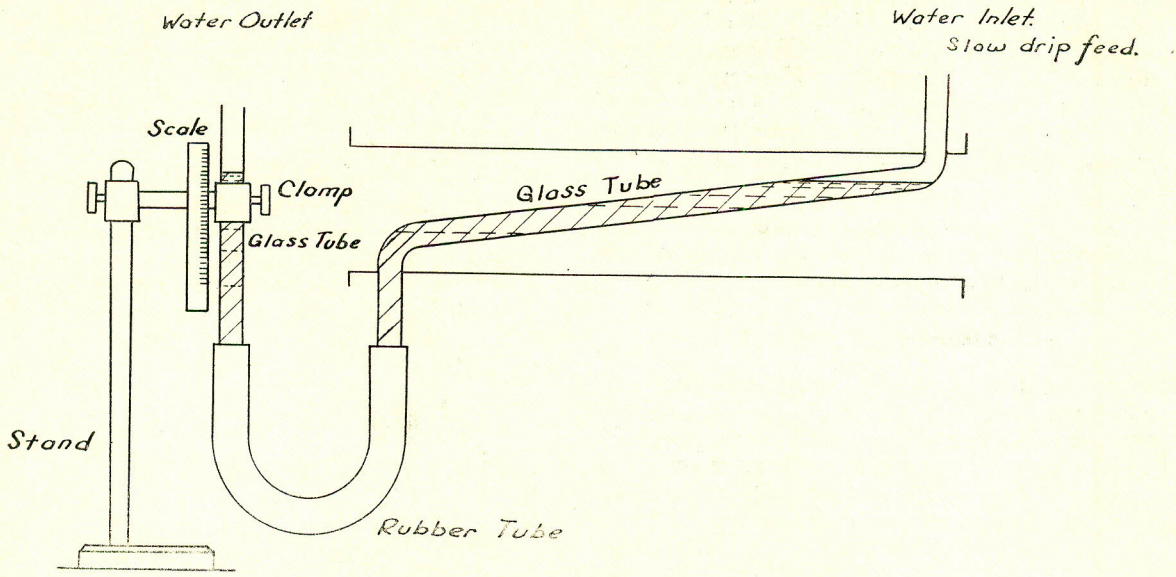

Fig. 8.—Schematic diagram of variable water load attenuator.

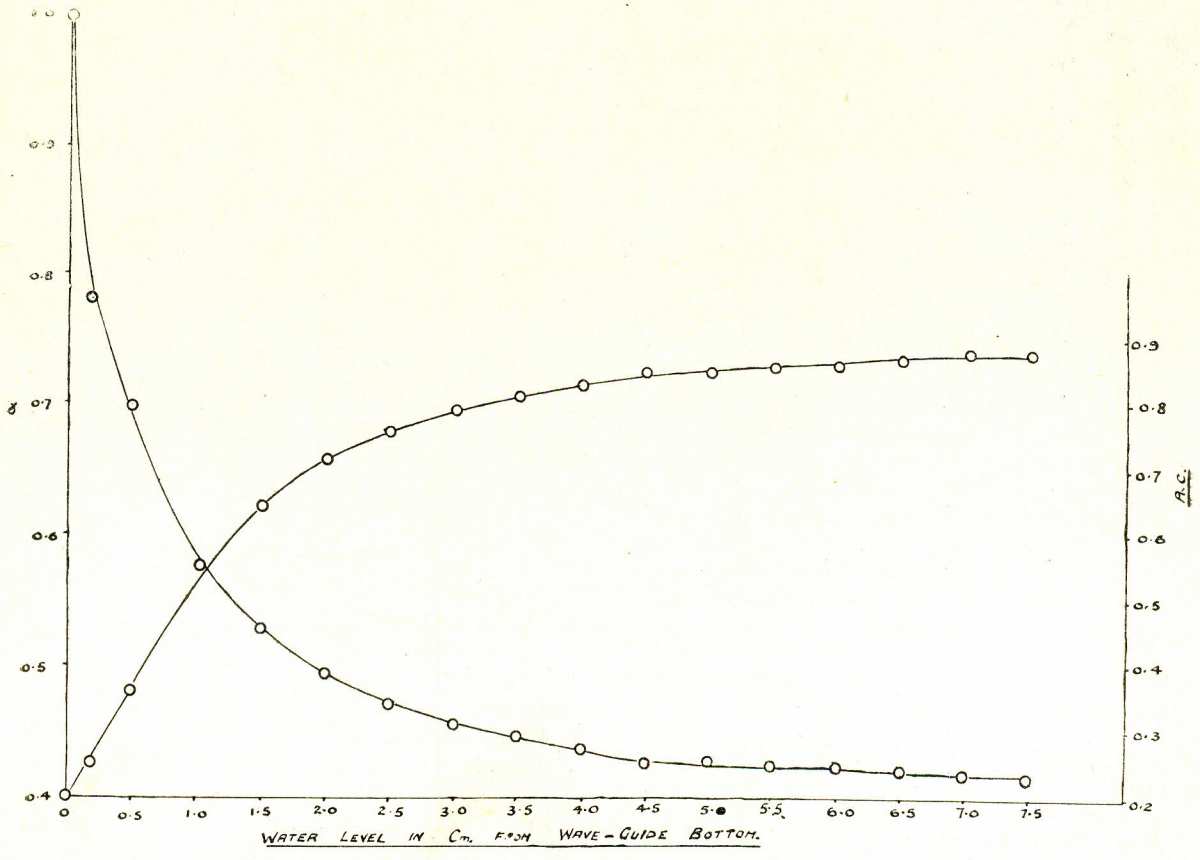

Fig. 9.—Attenuation of water load attenuator.

measurements. The results of measurements are shown in Figs. 9, 10(a) and 10(b).

The variation of attenuation with water level in the glass tube inside the attenuator was very smooth as shown in Fig. 9. The water had to be slowly dripped and care was taken to drive out any air bubbles in the water column inside the attenuator. The attenuation was dependent slightly on the frequency. This was due to the very broad resonance characteristics of a long waveguide. The reflection of electromagnetic waves from the attenuator was negligible.

The circle diagrams of the attenuator terminated by the cavity are given in Figs. 10(a) and (b) for $\alpha^2=0.25$, 0.5 and 0.75 respectively. These diagrams could easily be made symmetrical with respect to the centre of the impedance chart by putting a suitable quarter-wave transformer at the input of the attentuator. The circle diagram for $\alpha^2=0.5$ or $\alpha^2=0.75$ would be quite good, when made symmerrical for stabilization of magnetron frequency. Under this condition one-third of the input power would be dissipated in the attenuator which might be considered quite reasonable. The circle diagram for $\alpha^2=0.25$ or $\alpha^2=0.5$

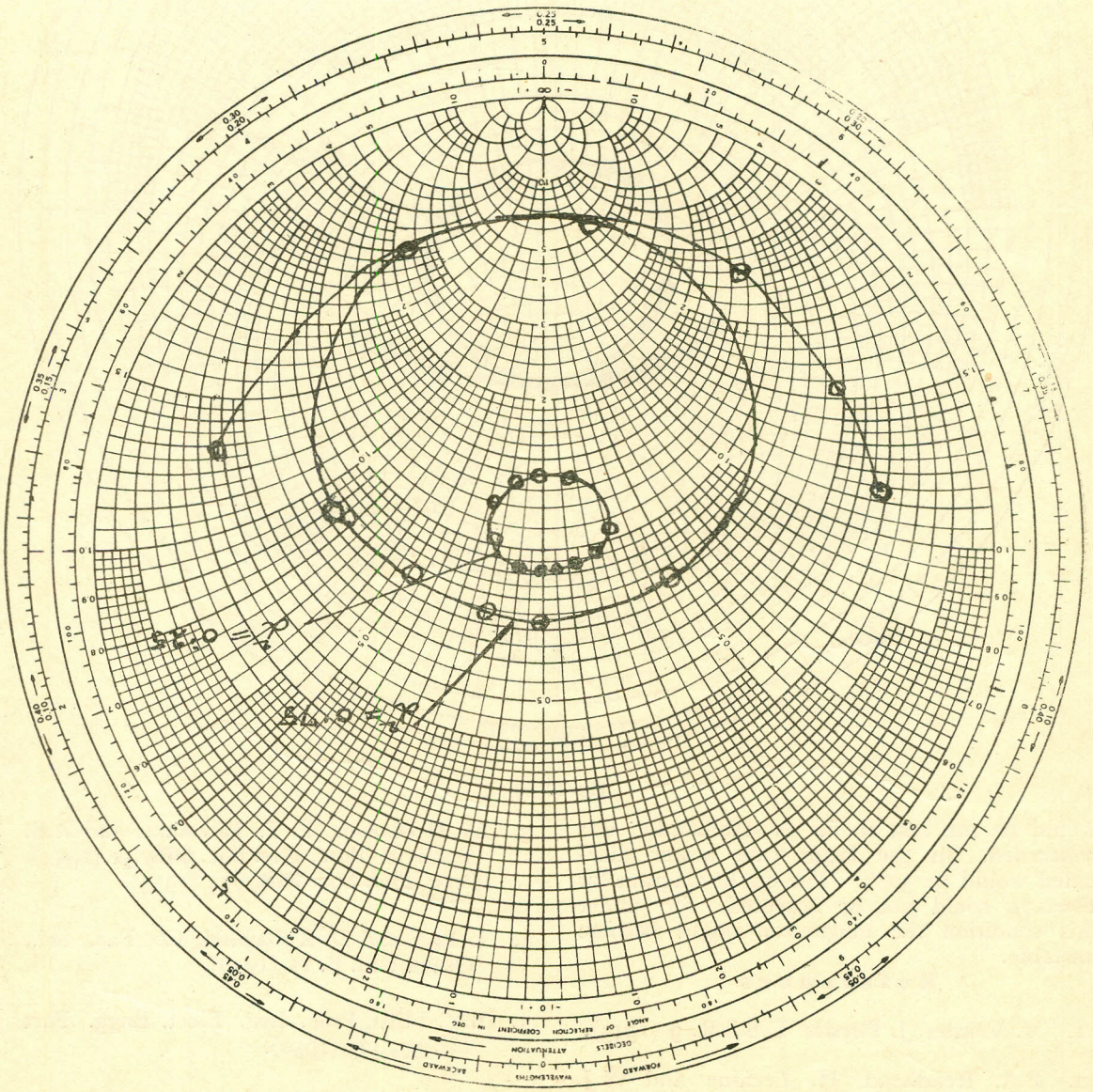

Fig. 10 (a)

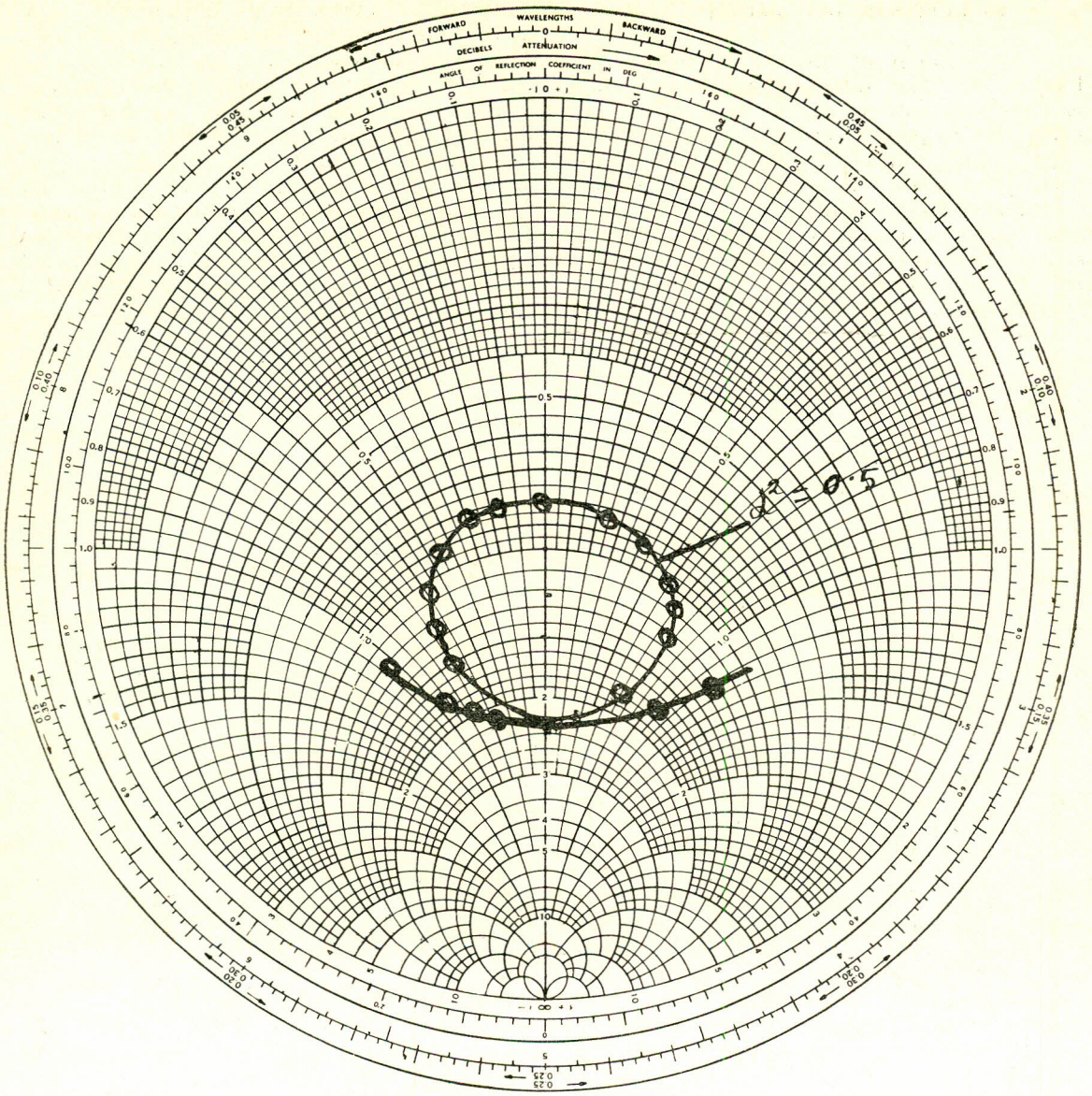

Fig. 10 (b)

would be the best so far as stabilization was concerned. In the latter case power dissipated would be 50%. The circle diagram for $\alpha^2=0.75$ could not be accepted, for under this condition the magnetron might become unstable.

References

1. V. Veksler, J. Physics U.S.S.R. **9** (1945).
2. P.A. Readhead, H. Lecaine and W.J. Henderson, Canadian Journal of Research, A, **28** (1950).
3. C. Herderson, F. F. Heymann and R.E. Jennigus, Proc. Phy. Soc. **66B, 41** (1953). Proc. Phy. Soc. **66B,** 654 (1953).
4. I. Itoh and D. Kobayashi, Co. Fac. Sci., Osaka Uni. B. **11** (1950).
5. B.Y. Mills, Proc. Inst. Elect. Engg. Part III, **97,** 425 (1950).
6. L.G. Huxley, *Wave-guides* (Cambridge 1947).